

Internal power loss in GaN-based lasers: mechanisms and remedies

Joachim Piprek¹ 

Received: 21 August 2017 / Accepted: 13 September 2017
© Springer Science+Business Media, LLC 2017

Abstract GaN-based laser diodes transform only a relatively small fraction of the electrical input power into laser light. The inherently large series resistance of these devices causes significant self-heating that leads to the typical power roll-off at high current. We analyze recently reported measurements using advanced numerical laser simulation and investigate the physical mechanisms that limit the lasing power in continuous-wave operation. Contrary to common expectations, our analysis reveals a strong influence of Auger recombination since the self-heating leads to a rising quantum well carrier density above the lasing threshold. As possible remedy, we investigate the effect of a tunnel-junction contact and predict a significant enhancement of lasing power and efficiency.

Keywords Laser diode · InGaN/GaN · Power · Efficiency · Auger recombination · Series resistance · Joule heating · Hole conductivity · Tunnel junction

1 Introduction

GaN-based light emitting diodes (LEDs) transform up to 84% of the electrical input power into light output power (Hurni et al. 2015) while GaN-based lasers reach less than half of that power conversion efficiency (Strauss et al. 2017). On the other hand, GaN-LEDs suffer from strongly sub-linear power versus current characteristics that are observed across the

This article is part of the Topical Collection on Numerical Simulation of Optoelectronic Devices, NUSOD'17.

Guest edited by Matthias Auf der Maur, Weida Hu, Slawomir Sujecki, Yuh-Renn Wu, Niels Gregersen, Paolo Bardella.

✉ Joachim Piprek
piprek@nusod.org

¹ NUSOD Institute LLC, Newark, DE 19714-7204, USA

entire wavelength spectrum. Recent research indicates that this LED efficiency droop is mainly caused by Auger recombination inside the InGaN quantum wells (QWs) (Weisbuch et al. 2015). Auger recombination rises with the third power of the QW carrier density and therefore intensifies with stronger current injection into the LED. In contrast, InGaN/GaN laser diodes are expected to suffer less from Auger recombination, based on the common assumption that the QW carrier density does not rise with increasing current injection above the lasing threshold (Wierer and Tsao 2015; Cantore et al. 2015). In Nakamura (2015) the author stated that “Auger recombination, with the resulting efficiency droop, does not appreciably occur in blue laser diodes”. Considering the self-heating of laser diodes, our paper challenges these assumptions by advanced numerical analysis of recent measurements on high-power InGaN/GaN lasers. As possible remedy, we also study the insertion of a tunnel junction which reduces self-heating and Auger recombination.

2 Models and parameters

Our analysis employs the commercial laser simulation software PICS3D by Crosslight Software Inc. which self-consistently combines carrier transport, QW band structure, stimulated photon emission, wave guiding, and heat flow. Schrödinger and Poisson equations are solved iteratively in order to account for the QW deformation with changing device bias due to the built-in polarization field (quantum-confined Stark effect). The transport model includes Fermi statistics, drift and diffusion of electrons and holes, interband tunneling as well as carrier loss mechanisms such as Shockley–Read–Hall (SRH) recombination, spontaneous photon emission, Auger recombination, and carrier leakage. More details on the laser model are published elsewhere (Piprek and Nakamura 2002; Piprek 2003).

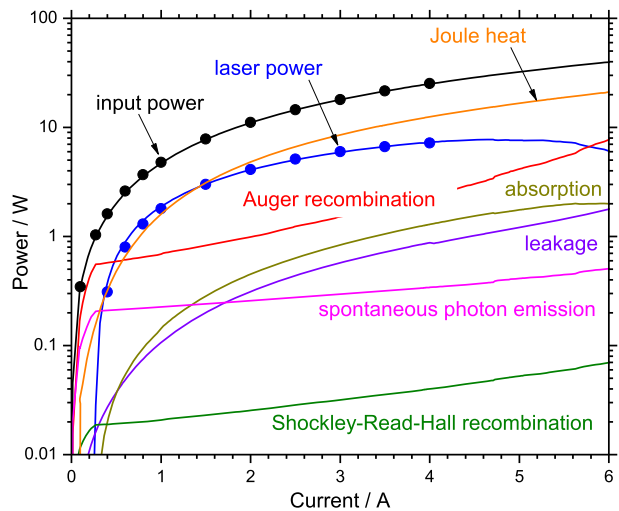
As practical example we analyze recently published experimental results for InGaN/GaN Fabry–Perot laser diodes demonstrating a maximum light output power of $P = 7.2$ W at $I = 4$ A injection current in continuous-wave (CW) operation at room temperature (Kawaguchi et al. 2016). This record-high lasing power is based on an optimized ridge-waveguide structure with strongly reduced internal absorption ($\alpha_i = 2.5/\text{cm}$) as well as on a low thermal resistance of about 7 K/W (Nozaki et al. 2016). However, due to the large series resistance, a high bias of $V = 6.3$ V was measured at 4 A which is about double the bias required by the photon energy (Piprek 2017b).

The layer structure is given in Table 1. The electron blocking layer (EBL) was moved to the p-side edge of the waveguide in order to minimize the bias (Kawaguchi et al. 2016). Key material parameters are obtained by simulating the measured laser performance (dots in Fig. 1). The threshold current is mainly controlled by QW Auger recombination with a temperature-independent coefficient $C = 4.3 \times 10^{-30} \text{ cm}^6/\text{s}$, which lies within the range of reported numbers (Piprek et al. 2015). Defect-related SRH recombination has a negligible impact despite the relatively short SRH lifetime of 20 ns assumed inside the QWs. The slope efficiency is mainly limited by free-carrier absorption (Kawaguchi et al. 2016). We adopt a first-principle model for phonon-assisted free-carrier absorption which results in an absorption cross section of about $0.6 \times 10^{-18} \text{ cm}^2$ for our case (Kioupakis et al. 2010). Without further fitting, these parameters give good agreement with the measured laser power in Fig. 1. The measured bias V and input power IV (Fig. 1) are reproduced by calibrating the p-cladding hole mobility ($2 \text{ cm}^2/\text{Vs}$) and the p-contact resistance

Table 1 Simulated laser structure (Kawaguchi et al. 2016)

Layer	Composition	Thickness (nm)	Refractive index
p-cladding	$\text{Al}_{0.026}\text{Ga}_{0.974}\text{N:Mg}$	660	2.520
p-EBL	$\text{Al}_{0.36}\text{Ga}_{0.64}\text{N:Mg}$	5	2.350
Waveguide	GaN	250	2.528
Waveguide	$\text{In}_{0.008}\text{Ga}_{0.992}\text{N}$	100	2.522
Quantum well	$\text{In}_{0.066}\text{Ga}_{0.934}\text{N}$	7.5	2.622
Barrier	$\text{In}_{0.008}\text{Ga}_{0.992}\text{N}$	20	2.522
Quantum well	$\text{In}_{0.066}\text{Ga}_{0.934}\text{N}$	7.5	2.622
Waveguide	$\text{In}_{0.008}\text{Ga}_{0.992}\text{N}$	40	2.522
Waveguide	GaN	450	2.528
n-cladding	$\text{Al}_{0.026}\text{Ga}_{0.974}\text{N:Si}$	900	2.520

The ridge waveguide is 12 μm wide and the cavity is 1.2 mm long with facet reflectivities of 0.056 and 0.95, respectively. External electrical and thermal resistances are added in the simulation to find agreement with the measurements

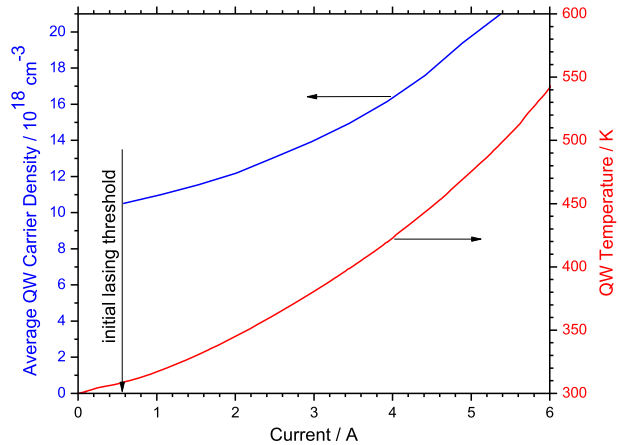
Fig. 1 Simulated power components (dots: measurement)

($R_c = 0.35 \Omega$). Both numbers are not reported for this laser but our results are close to literature data (Yonkee et al. 2016).

3 Power loss mechanisms

Figure 1 plots the calculated power components versus injection current. Joule heating represents the largest power loss at higher current. It is mainly rooted in the low p-AlGaIn hole conductivity and the large p-contact resistance (Piprek 2017b). The QW temperature rises by $\Delta T = 122 \text{ K}$ at $I = 4 \text{ A}$ (Fig. 2) in good agreement with the measured thermal resistance. This self-heating reduces the QW gain so that the QW carrier density needs to

Fig. 2 Average carrier density and temperature inside the quantum wells



rise in order to maintain the threshold gain (Piprek 2017a). Figure 2 reveals that the QW carrier density grows by more than 50% at $I = 4$ A, relative to the initial threshold carrier density of about 10^{19} cm^{-3} . The rising QW carrier density leads to increasing carrier losses which are dominated by Auger recombination (Fig. 1). Electron leakage, spontaneous photon emission, and defect-related SRH recombination cause much smaller power losses. However, electron leakage triggers enhanced free-carrier absorption inside the p-side waveguide layers which severely limits the maximum lasing power (Piprek 2017b). Thus, Joule heating, Auger recombination, and electron leakage are the reasons for the low output power of GaN-based lasers.

4 Tunnel-junction laser

Obviously, reduction of the Joule heating by enhancing the p-side electrical conductivity is the most promising strategy to increase the lasing power. Less self-heating leads to lower QW carrier densities which also reduces all other power losses. In the following, we therefore investigate the inclusion of a tunnel-junction contact in our laser structure (Yonkee et al. 2016). Our tunnel-junction design replaces part of the highly resistive p-doped AlGaIn cladding layer by highly conductive n-doped AlGaIn (Fig. 3). In order to predict the ultimate performance of such design, we assume that both the tunnel junction resistance and the n-AlGaIn contact resistance are negligibly small.

Figure 4 compares calculated bias versus current characteristics. Removal of the p-contact resistance R_c from the original laser simulation already reduces the bias significantly. The corresponding dash-dot curve in Fig. 4 also reveals the temperature sensitivity of the remaining p-AlGaIn cladding resistance. The 122 K temperature rise at $I = 4$ A nearly quadruples the p-cladding hole density in our simulation, due to the large Mg acceptor ionization energy of 178 meV. Such bias reduction at higher temperature was confirmed experimentally by current–voltage measurements at different stage temperatures (Strauss et al. 2017). In other words, at high currents, the series resistance is mainly determined by the p-contact and not by the p-cladding (Piprek 2017b). Therefore, additional insertion of the tunnel-junction mainly affects the bias at lower current (dashed line in Fig. 4).

Fig. 3 Electron band diagram for the simulated tunnel-junction laser

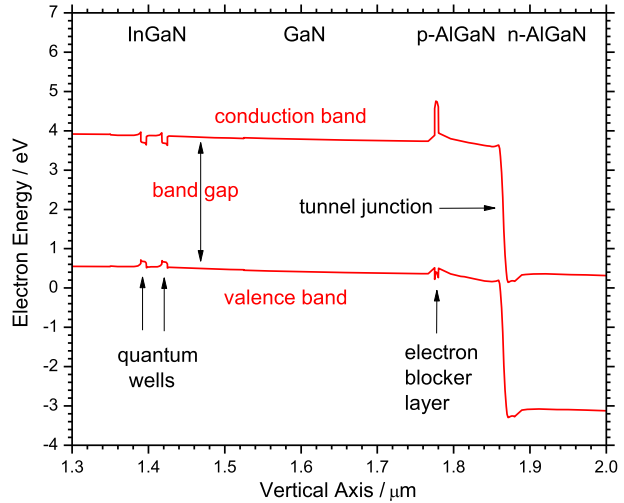
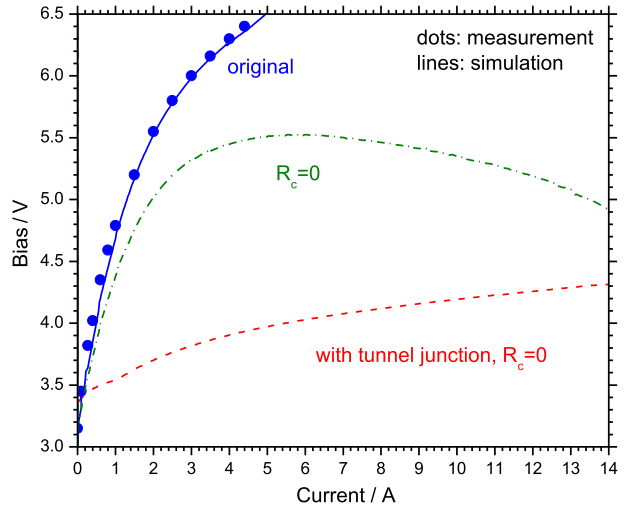
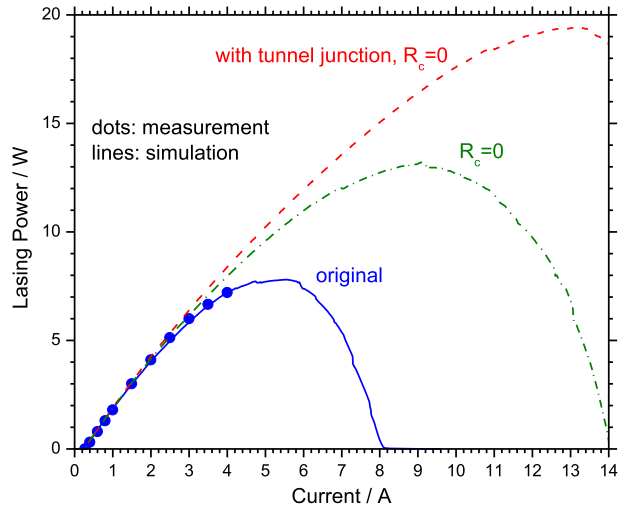


Fig. 4 Bias versus current calculated for the original structure (solid line), after removal of the contact resistance (dash-dot line), and after insertion of the tunnel junction (dashed line)



Consequently, the self-heating of the laser is also reduced. At 4 A injection current, the QW temperature rises by only 81 K without contact resistance and by only 40 K with added tunnel junction. Lower self-heating translates into a smaller QW carrier density and less carrier loss. The resulting lasing powers are compared in Fig. 5. The peak power rises dramatically, from 7 to 13 W after removal of the p-contact resistance, and to 19 W after insertion of the tunnel junction.

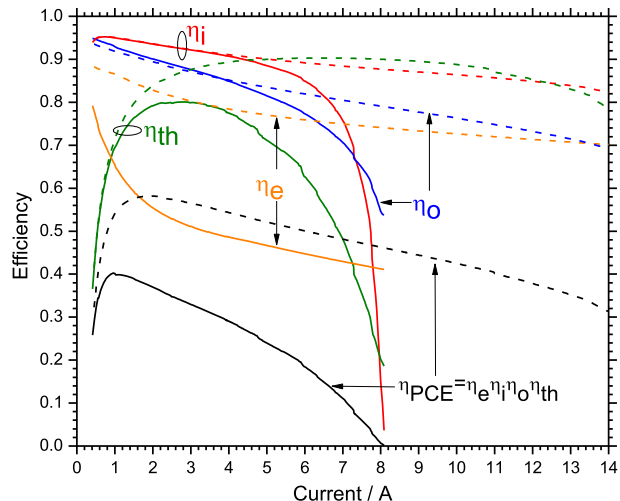
Fig. 5 Laser power versus current calculated for the original structure (solid line), after removal of the contact resistance (dash-dot line), and after insertion of the tunnel junction (dashed line)



5 Efficiency comparison

Our efficiency comparison is based on the approach previously introduced for the original device (Piprek 2017a). The power conversion efficiency (PCE) is defined as ratio of laser output power to electrical input power and it can be split up into four components: $\eta_{PCE} = \eta_e \eta_i \eta_o \eta_{th}$. The electrical efficiency η_e accounts for the large series resistance. The differential internal efficiency η_i is reduced by electron leakage from the quantum wells into the p-side waveguide layers where they contribute to the rising free-carrier absorption and the falling optical efficiency η_o (Piprek 2017b). The threshold current efficiency η_{th} reflects QW carrier losses that are dominated by Auger recombination. All these efficiencies are plotted in Fig. 6 for both laser designs and are discussed in the following.

Fig. 6 Calculated efficiencies of the original laser (solid lines) and the tunnel-junction laser w/o contact resistance (dashed lines). η_{PCE} , overall power conversion efficiency; η_e , electrical efficiency; η_o , optical efficiency; η_i , differential internal efficiency; η_{th} , threshold current efficiency



The PCE of the original laser is mainly affected by the large series resistance (η_e) but Auger recombination (η_{th}) gains increasing influence with higher injection current and higher QW temperature. Contrary to common expectations, a strong PCE droop starts already at 1 A injection current. Figure 6 reveals that this efficiency droop is caused by the declining electrical efficiency η_e while the threshold current efficiency η_{th} is still rising at the PCE peak. However, the maximum lasing power is mainly controlled by Auger recombination which dominates the strongly decreasing threshold current efficiency η_{th} at higher current.

The tunnel-junction laser exhibits a significant improvement of the electrical efficiency η_e due to the reduced bias. At 4 A current, η_e rises from the original 49 to 78%. At the same current, the threshold current efficiency η_{th} is enhanced from 77 to 89% due to the lower threshold carrier density and reduced Auger recombination. Internal differential efficiency and optical efficiency don't change much at this current, i.e., electron leakage and the resulting free-carrier absorption are hardly affected by the tunnel junction. The tunnel junction is located in the tail region of the optical mode and therefore causes little additional absorption, which is only visible in a slight reduction of the optical efficiency η_o at low current in Fig. 6. Multiplication of all four efficiencies gives the PCE, whose peak value of 58% is well above the original 39%. The subsequent efficiency droop is smaller than before. The PCE is still 45% at 8 A injection current and 15 W output power, which is double of the original peak power.

6 Summary

In summary, advanced numerical analysis of laser measurements reveals a strong influence of Joule heating and Auger recombination on the output power of InGaN/GaN lasers. The insertion of a p-side tunnel junction and the removal of the p-contact resistance promise significant power and efficiency enhancements.

References

- Cantore, M., Pfaff, N., Farrell, R.M., Speck, J.S., Nakamura, S., DenBaars, S.P.: High luminous flux from single crystal phosphor-converted laser-based white lighting system. *Opt. Express* **24**, 251040 (2015)
- Hurni, C.A., David, A., Cich, M.J., Aldaz, R.I., et al.: Bulk GaN flip-chip violet light-emitting diodes with optimized efficiency for high-power operation. *Appl. Phys. Lett.* **106**, 031101 (2015)
- Kawaguchi, M., Imafuji, O., Nozaki, S., Hagino, H., et al.: Optical-loss suppressed InGaN laser diodes using undoped thick waveguide structure. *Proc. SPIE* **9748**, 974818 (2016)
- Kioupakis, E., Rinke, P., Van de Walle, C.: Determination of internal loss in nitride lasers from first principles. *Appl. Phys. Express* **3**, 082101 (2010)
- Nakamura, S.: Background story of the invention of efficient blue InGaN light emitting diodes (Nobel Lecture). *Ann. Phys.* **527**, 335–349 (2015)
- Nozaki, S., Yoshida, S., Yamanaka, K., Imafuji, O., et al.: High-power and high-temperature operation of an InGaN laser over 3 W at 85 °C using a novel double-heat-flow packaging technology. *Jpn. J. Appl. Phys.* **55**, 04EH05 (2016)
- Piprek, J.: *Semiconductor Optoelectronic Devices: Introduction to Physics and Simulation*. Academic, San Diego (2003)
- Piprek, J.: What limits the efficiency of high-power InGaN/GaN lasers? *J. Quant. Electron.* **53**, 2000104 (2017a)
- Piprek, J.: What limits the power conversion efficiency of GaN-based lasers? *Proc. SPIE* **10098**, 100980Q (2017b)

- Piprek, J., Nakamura, S.: Physics of high-power InGaN/GaN lasers. *IEE Proc. Optoelectron.* **149**, 145–151 (2002)
- Piprek, J., Roemer, F., Witzigmann, B.: On the uncertainty of the Auger recombination coefficient extracted from InGaN/GaN light-emitting diode efficiency droop measurements. *Appl. Phys. Lett.* **106**, 101101 (2015)
- Strauss, U., Somers, A., Heine, U., Wurm, T., et al.: GaInN laser diodes from 440 to 530 nm: a performance study on single mode and multi-mode R&D designs. *Proc. SPIE* **10123**, 101230A (2017)
- Weisbuch, C., Piccardo, M., Martinelli, L., Iveland, J., Peretti, J., Speck, J.S.: The efficiency challenge of nitride light-emitting diodes for lighting. *Phys. Status Solidi A* **212**, 899–913 (2015)
- Wierer, J.J., Tsao, J.Y.: Advantages of III-nitride laser diodes in solid-state lighting. *Phys. Status Solidi A* **212**(5), 980–985 (2015)
- Yonkee, B.P., Young, E.C., Lee, C., Leonard, J.T., et al.: Demonstration of a III-nitride edge-emitting laser diode utilizing a GaN tunnel junction contact. *Opt. Express* **24**, 256556 (2016)